Binuclear Complexes of Macrocyclic Ligands. Electrochemical and Spectral Properties of Homobinuclear $Cu^{II}Cu^{II}$, $Cu^{II}Cu^{I}$, and $Cu^{I}Cu^{I}$ Species Including an Estimated Intramolecular Electron Transfer Rate

Robert R. Gagné,* Carl A. Koval, Thomas J. Smith, and Marc C. Cimolino

Contribution No. 5928 from the Division of Chemistry and Chemical Engineering, California Institute of Technology, Pasadena, California 91125.
Received December 18, 1978

Abstract: Electrochemical techniques were employed to study electron transfer properties of a binuclear copper-macrocyclic ligand complex and to prepare several reduced derivatives. The complex, $Cu^{II}Cu^{II}L(ClO_4)_2 \cdot 2H_2O$, was prepared by condensing 1,3-diaminopropane with 5-methyl-2-hydroxyisophthalaldehyde and $Cu(ClO_4)_2 \cdot 6H_2O$. The $Cu^{II}Cu^{II}$ complex was reduced in successive, quasi-reversible, one-electron steps at −0.52 and −0.91 V vs. NHE. Constant-potential electrolysis was employed to prepare the reduced species, $Cu^{II}Cu^{I}L(ClO_4)$ and $Cu^{I}Cu^{I}L$, both of which were isolated and fully characterized. The mixed-valence species, $Cu^{II}Cu^{I}L^{+}$, is stable in oxygen-free solutions (conproportionation constant: 3.97×10^6) and reacts with carbon monoxide to form an adduct, $Cu^{II}Cu^{I}L(CO)ClO_4$. The diamagnetic $Cu^{I}Cu^{I}L$ species was obtained as essentially insoluble black needles which, however, formed a soluble dicarbonyl adduct, $Cu^{I}Cu^{I}L(CO)_2$, on exposure to CO. The latter complex was not isolated. At the ambient temperature $Cu^{II}Cu^{I}L^{+}$ exhibits an isotropic seven-line solution EPR spectrum while an anisotropic pattern was observed in frozen solutions (77 K), with four lines for $g_{\parallel}$ and unresolved $g_{\perp}$. Variable-temperature experiments indicated coalescence at about 200 K suggesting an intramolecular electron transfer rate of about 1.7×10^{10} s^{-1} at 298 K. Electronic absorption spectral measurements revealed at least two absorptions for $Cu^{II}Cu^{I}L(ClO_4)_2$ at 1700 and 1200 nm (CH_2Cl_2), which are not present in $Cu^{II}Cu^{II}L(ClO_4)_2 \cdot 2H_2O$, $Cu^{I}Cu^{I}L$, or the carbonyl derivatives. The new spectral bands may be attributable to intramolecular electron transfer processes.

Introduction

In this paper we report the synthesis and characterization of the $Cu^{II}Cu^{I}$ and $Cu^{I}Cu^{I}$ derivatives which are formed upon reduction of a previously reported $Cu^{II}Cu^{II}$ macrocyclic ligand complex.[1] The mixed-valence ion, $Cu^{II}Cu^{I}L^{+}$, exhibits an unusual electronic absorption spectrum and temperature-dependent EPR spectra which permit a reasonable estimate of the intramolecular electron transfer rate. Properties of the mixed-valence ion, $Cu^{II}Cu^{I}L^{+}$, will be compared to those of other well-characterized mixed-valence species.

A drawing of the parent $Cu^{II}Cu^{II}$ complex and the derivatives reported herein, along with the nomenclature used throughout this paper, is presented in Figure 1. A preliminary account of this work has already appeared.[5]

Results

Electrochemistry and Synthesis. The binuclear complex, $Cu^{II}Cu^{II}L(ClO_4)_2 \cdot 2H_2O$, was prepared by condensing 1,3-diaminopropane with 5-methyl-2-hydroxyisophthalaldehyde and $Cu(ClO_4)_2 \cdot 6H_2O$ according to the method of Pilkington and Robson.[2] Under an inert atmosphere, $Cu^{II}Cu^{II}L^{2+}$ can be reduced electrochemically to $Cu^{II}Cu^{I}L^{+}$ and $Cu^{I}Cu^{I}L$ in separate one-electron processes. If a CO atmosphere is used, $Cu^{II}Cu^{II}L^{2+}$ can be reduced stepwise to $Cu^{II}Cu^{I}L(CO)^{+}$ and $Cu^{I}Cu^{I}L(CO)_2$. These processes, outlined in Tables I and II and in Figure 2, are all reversible or quasi-reversible. The observed electrochemistry is, however, often complicated by the very low solubility of $Cu^{I}Cu^{I}L$. The top of Figure 3 contains cyclic voltammograms of $Cu^{II}Cu^{II}L^{2+}$ in CH_3CN under N_2 at a platinum electrode. Two reduction processes are evident, occurring at approximately −0.45 and −0.90 V. If the potential scan is reversed at −0.75 V, the wave at −0.40 V is quasi-reversible. The wave at ~−0.95 V does not have the characteristic shape of a diffusion-controlled process.[7] The oxidation waves associated with this reduction, located at ~−0.65 and −0.42 V, are also misshapen. There is little difference between voltammograms recorded using a HMDE[6] or a platinum electrode except in the shape of the two distorted oxidation waves. The compound $Cu^{II}Cu^{II}L^{2+}$ is not highly soluble in CH_2Cl_2, CH_3OH, or acetone containing 0.1 M TBAP.[6] Nevertheless, cyclic voltammograms of saturated solutions of $Cu^{II}Cu^{II}L^{2+}$ in these solvents resemble those shown in the top of Figure 3.

The compound $Cu^{I}Cu^{I}L$ is essentially insoluble in CH_3CN, CH_2Cl_2, and CH_3OH, and it is this insolubility which is responsible for the irreversibility of the reduction of $Cu^{II}Cu^{I}L^{+}$ to $Cu^{I}Cu^{I}L$. This compound is slightly soluble in DMF,[6] and a cyclic voltammogram of $Cu^{II}Cu^{II}L^{2+}$ in this solvent is shown in the bottom of Figure 3. Both reductions are now quasi-reversible, at least at moderately fast scan rates. At slower scan rates (0.1 V/s), cyclics in DMF begin to resemble the top of Figure 3. Under a CO atmosphere, cyclic voltammograms of $Cu^{II}Cu^{II}L^{2+}$ in any solvent are similar to the one in the bottom of Figure 3. This is because the CO adduct of $Cu^{I}Cu^{I}L$, $Cu^{I}Cu^{I}L(CO)_2$, is appreciably soluble.

Owing, at least in part, to uncompensated solution resistance, the peak separations for the various quasi-reversible cyclic voltammograms of $Cu^{II}Cu^{II}L^{2+}$ were no smaller than 70 mV and the separations increased with increasing scan rate. For this reason cyclic voltammetry was not used to evaluate formal reduction potentials. Nevertheless, values of E^f calculated using the formula $E^{f\,6} = (E_{p_a} + E_{p_c})/2$ were close to those obtained using other techniques.

The n values for the four processes shown in the scheme were found to be 1.0 ± 0.1 by constant-potential electrolysis in DMF and CH_3CN. Millimolar solutions could be repeatedly reduced and reoxidized without loss of material. As expected, when $Cu^{I}Cu^{I}L$ was created as an electrolysis product it was nearly insoluble, forming a precipitate at a Hg pool and coating a Pt gauze electrode with a shiny black film. Constant-potential electrolysis of more concentrated solutions of $Cu^{II}Cu^{II}L^{2+}$ was the basis for the synthesis of $Cu^{II}Cu^{I}L(ClO_4)$, $Cu^{II}Cu^{I}L(CO)ClO_4$, and $Cu^{I}Cu^{I}L$. The procedures, which are detailed in the Experimental Section, are outlined in Figure

0002-7863/79/1501-4571$01.00/0

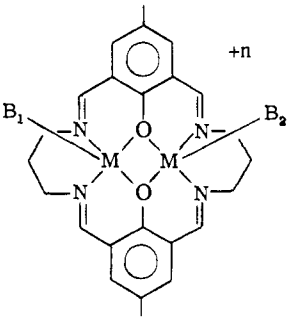

Complex	B_1	B_2
$Cu(II)Cu(II)L^{+2}$	—	—
$Cu(II)Cu(I)L^{+}$	—	—
$Cu(II)Cu(I)L(CO)^{+}$	—	CO
Cu(I)Cu(I)L	—	—
$Cu(I)Cu(I)L(CO)_2$	CO	CO
$Zn(II)Zn(II)L^{+2}$	—	—

Figure 1. Schematic drawing and nomenclature of the binuclear complexes studied.

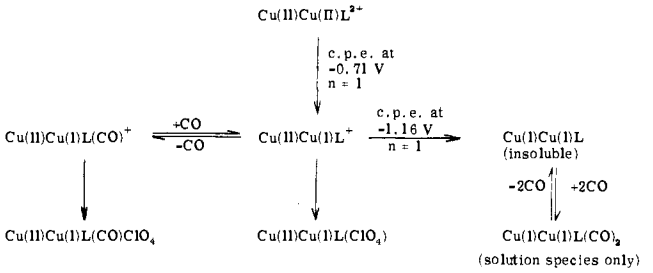

Figure 2. Synthesis of the reduced forms of $Cu^{II}Cu^{II}L(ClO_4)_2 \cdot 2H_2O$.

2. Stoichiometries for the addition of CO to $Cu^{II}Cu^{I}L(ClO_4)$ and $Cu^{I}Cu^{I}L$ were determined by adding weighed quantities of these compounds to DMF and recording the subsequent uptake of CO. As indicated in Figure 2, $Cu^{II}Cu^{I}L(ClO_4)$ absorbed 1.0 ± 0.05 mol of CO per mol of complex and the uptake for $Cu^{I}Cu^{I}L$ was 2.0 ± 0.1. The compounds $Cu^{II}Cu^{I}L(ClO_4)$ and $Cu^{I}Cu^{I}L$ could be prepared as crystalline materials, while $Cu^{II}Cu^{I}L(CO)ClO_4$ formed a microcrystalline powder. Attempts to isolate the dicarbonyl complex, $Cu^{I}Cu^{I}L(CO)_2$, from solution led only to reisolation of the far less soluble complex, $Cu^{I}Cu^{I}L$.

The reduction of $Cu^{II}Cu^{II}L^{2+}$ in DMF was also investigated using dc polarography. Polarographic data are summarized in Table I. Again, the insolubility of $Cu^{I}Cu^{I}L$ caused the wave associated with the reduction of $Cu^{II}Cu^{I}L^{+}$ to $Cu^{I}Cu^{I}L$ to be distorted. The reduction of $Cu^{II}Cu^{II}L^{2+}$ to $Cu^{II}Cu^{I}L^{+}$ and to $Cu^{II}Cu^{I}L(CO)^{+}$, however, gave reversible waves as judged by the slope of $-E$ vs. $\log i/(i_d - i)$ plots which should be 58 mV at 23 °C for a one-electron process.[8] Also included in Table I are data for the reductions of O_2, Cu^{II}(saltn), and $Zn^{II}Zn^{II}L^{2+}$. The complex Cu(saltn) might be considered as a monomer for $Cu^{II}Cu^{II}L^{2+}$, but the difference in charge causes

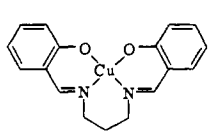

Cu(II)(saltn)

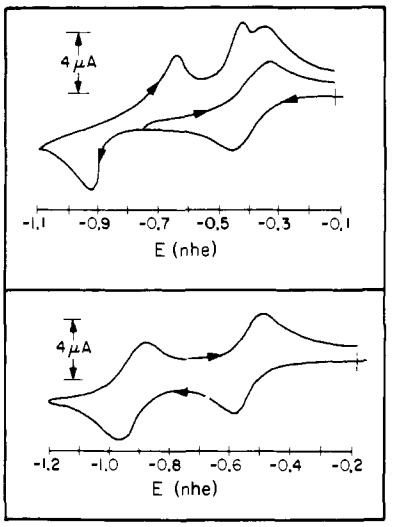

Figure 3. Cyclic voltammograms of $Cu^{II}Cu^{II}L^{2+}$ (~1 mM) under an inert atmosphere. Top: in CH_3CN; scan rate of 1 V/s. Bottom: in DMF; scan rate of 3 V/s.

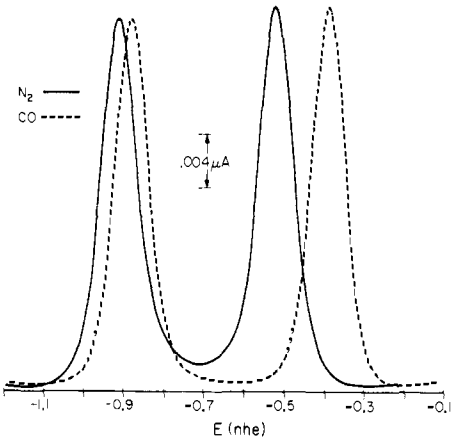

Figure 4. Differential pulse voltammograms of $Cu^{II}Cu^{II}L^{2+}$ ($\sim 5 \times 10^{-5}$ M, DMF).

its reduction to occur nearly 0.6 V cathodic of the reduction of $Cu^{II}Cu^{II}L^{2+}$ to $Cu^{II}Cu^{I}L^{+}$. As expected, since $Zn^{II}Zn^{II}L^{2+}$ contains no Cu^{II} atom, it was not easily reduced. The reduction of oxygen to superoxide ion was not reversible in DMF on Hg, but its half-wave potential is provided as a reference point.

In order to avoid solubility problems, differential pulse voltammetry (DPV) was used to investigate dilute solutions of $Cu^{II}Cu^{II}L^{2+}$ in DMF. Figure 4 contains DPV scans of $Cu^{II}Cu^{II}L^{2+}$ on platinum under both nitrogen and carbon monoxide atmospheres. The peak potentials, E_p, from this figure are in Table II along with half-wave potentials that can be calculated using the formula[9]

$$E_{1/2} = E_p + \frac{MA}{2}$$

where MA is the modulation amplitude or pulse height. Also included are the peak widths at half-height, $\Delta E_{1/2i}$, which are close to the theoretical value of $90.4/n$ mV.[9] The values of $E_{1/2}$ and $E_{1/2}(CO)$ obtained by DPV agree with the polarographic values within a few millivolts.

If differences in diffusion coefficients between the oxidized and reduced halves of redox couples are ignored, values of $E_{1/2}$ obtained in the above electrochemical experiments can be used as the E^{f}'s shown in the scheme. Knowledge of these formal potentials enables one to quantify some interesting properties of the system. One is the conproportionation constant de-

Table I. Polarographic Data[a]

compd	atmosphere	$E_{1/2}$[b]	slope[c]	I_d[d]	comments
$Cu^{II}Cu^{II}L(ClO_4)_2 \cdot 2H_2O$	N_2	−0.517	57.8	1.34	first reduction only
	CO	−0.392	56.9	1.39	
$Zn^{II}Zn^{II}L(ClO_4)_2 \cdot 2H_2O$	N_2				no waves positive of −1.5 V
Cu^{II}(saltn)	N_2	−1.099	57.6	1.74	
	CO	−1.040	58.4	1.78	
O_2	N_2	−0.774	69.0		$O_2 + e^- \rightleftharpoons O_2^-$

[a] DMF[6] solution; $C \sim 0.5$ mM; TBAP[6] (0.1 M); scan rate = 0.5 mV/s. [b] Vs. NHE. [c] Of $-E$ vs. $\log i/(i_d - i)$ plot (mV). [d] $I_d = i_d/(m^{2/3}t^{1/6}C)$: i_d is the diffusion-limited current (μA); m is the flow rate (mg/s); t is the drop time (s); C is the concentration (mM).

Table II. Differential Pulse Voltammetric Data[a]

process	atmosphere	E_p[b]	$E_{1/2}$[c]	$\Delta E_{1/2}$;[d]
$Cu^{II}Cu^{II}L^{2+} + e^- \rightleftharpoons Cu^{II}Cu^{I}L^+$	N_2	−0.518	−0.523	94
$Cu^{II}Cu^{II}L^{2+} + e^- + CO \rightleftharpoons Cu^{II}Cu^{I}L(CO)^+$	CO	−0.387	−0.392	93
$Cu^{II}Cu^{I}L^+ + e \rightleftharpoons Cu^{I}Cu^{I}L$	N_2	−0.908	−0.913	94
$Cu^{II}Cu^{I}L(CO)^+ + e^- + CO \rightleftharpoons Cu^{I}Cu^{I}L(CO)_2$	CO	−0.876	−0.881	93

[a] DMF[6] solution; $C_b \sim 5 \times 10^{-5}$ M; TBAP[6] (0.1 M); scan rate = 2 mV/s; modulation amplitude (MA) = −10 mV. [b] Peak potential, vs. NHE. [c] $E_{1/2} = E_p + (MA/2)$; vs. NHE. [d] Peak width (mV) at half height.

Table III. EPR Parameters for the Mixed-Valence Compounds

sample	medium	temp, K	g_{av}	$g_\parallel$	$g_\perp$	$\lvert A_{av}\rvert \times 10^4$, cm^{-1}	$\lvert A_\parallel\rvert \times 10^4$, cm^{-1}
$Cu^{II}Cu^{I}L(ClO_4)$	solid	15	2.085				
	CH_3CN	298	2.262			42.25	
	CH_3CN	77		2.210	2.066		191.0
	CH_2Cl_2	298	2.169			45.57	
	CH_2Cl_2	82		2.228	2.080		187.3
	CH_3OH	292	2.069			38.64	
	$(CH_3)_2CO$	298	2 105			41.77	
$Cu^{II}Cu^{I}L(CO)ClO_4$	solid	77	2.089				
	CH_2Cl_2	298	2.113			83.86	
	CH_2Cl_2	79		2.224	2.073		197.3

scribing the equilibrium

$$Cu^{II}Cu^{II}L^{2+} + Cu^{I}Cu^{I}L \overset{K_{con}}{\rightleftharpoons} 2Cu^{II}Cu^{I}L^+$$

The value of K_{con} can be obtained from E_1^f and E_2^f using the formula

$$E_1^f - E_2^f = 0.0591 \log K_{con}$$

The value so calculated is $K_{con} = (4.0 \pm 0.1) \times 10^6$, using the data in Table II.

Figure 4 and the data in Tables I and II show that the presence of carbon monoxide causes the two reduction waves for $Cu^{II}Cu^{II}L^{2+}$ to shift anodically. The fact that compound $Cu^{II}Cu^{II}L^{2+}$ itself does not interact with CO, together with other evidence presented in this paper and in previous work,[10,11] indicates that the shifts are due to the binding of CO to Cu^I. Using the formal potentials measured at a CO concentration corresponding to 1 atm, $E^f_{(CO)}$, certain binding constants can be calculated. Because compound $Cu^{II}Cu^{I}L^+$ binds a single CO, the equilibrium constant for the reaction

$$Cu^{II}Cu^{I}L^+ + CO \overset{K_{CO}}{\rightleftharpoons} Cu^{II}Cu^{I}L(CO)^+$$

can be found using the equation[10,11]

$$E^f_{(CO)} - E_1^f = 0.059 \log (1 + K_{CO}[CO])$$

The value calculated using the data in Table I is $K_{CO} = (2.8 \pm 0.2) \times 10^4$. Assuming that the reduced form of Cu(saltn) also binds a single CO, the above formula yields a CO binding constant of $(2.0 \pm 0.3) \times 10^3$ for this unisolated Cu^I complex. Equilibrium constants for the binding of the first and second CO's to $Cu^{I}Cu^{I}L$ cannot be obtained from an electrochemical measurement at a single CO concentration.

Infrared Spectra. The infrared spectra of $Cu^{II}Cu^{I}L(ClO_4)$ and $Cu^{II}Cu^{I}L(CO)ClO_4$ are are similar to that of $Cu^{II}Cu^{II}L(ClO_4)_2 \cdot 2H_2O$, which is evidence that the ligand L is intact and unreduced in the new materials.[2,12] The spectrum of $Cu^{I}Cu^{I}L$ necessarily lacks bands due to ClO_4^- but otherwise closely resembles the other spectra. The carbonyl stretching frequency for $Cu^{II}Cu^{I}L(CO)ClO_4$ occurs at 2065 cm^{-1} in the solid state and at 2074 cm^{-1} in DMF solution. Although $Cu^{I}Cu^{I}L(CO)_2$ contains two carbonyls, only a single CO stretch is observed at 2061 cm^{-1} in the solution IR spectrum (DMF). The values for ν_{CO} are similar to those reported for other known Cu^I carbonyls.[10,13]

EPR. X-Band EPR spectra for $Cu^{II}Cu^{I}L(ClO_4)$ and $Cu^{II}Cu^{I}L(CO)ClO_4$ were obtained under a variety of conditions, as summarized in Table III. Spectra of $Cu^{II}Cu^{I}L^+$ in various solvents (CH_2Cl_2, CH_3CN, CH_3OH, and $(CH_3)_2CO$) at room temperature display a seven-line isotropic pattern in the $g = 2$ region with a separation of 40-45 G (Figure 5). The splitting arises from hyperfine interaction between the odd electron and two copper nuclei ($I = 3/2$). Exposure of CH_2Cl_2 solutions of $Cu^{II}Cu^{I}L^+$ to carbon monoxide leads to a four-line isotropic spectrum of the carbonyl adduct (Figure 5) for which the hyperfine splitting is now 85 G and is due to localization of the electron at a single copper site. Dissolution of $Cu^{II}Cu^{I}L(CO)ClO_4$ in CH_2Cl_2 under a helium atmosphere results in seven-line spectra characteristic of solution spectra of $Cu^{II}Cu^{I}L^+$ confirming that coordinated CO is readily released in solution. The magnitude of the splittings in the four-line case is typical for an electron localized on a single copper site while a splitting of 42 G has also been noted in the seven-line spectrum of a mixed-valence Cu^{II}/Cu^{I} complex formed from $Cu^{I}(CH_3CN)_4^+$ and $Cu^{II}(H_2O)_6^{2+}$ (1:1) with acetate ion in methanol.[14,15] The occurrence of a value of A_{av} for $Cu^{II}Cu^{I}L^+$

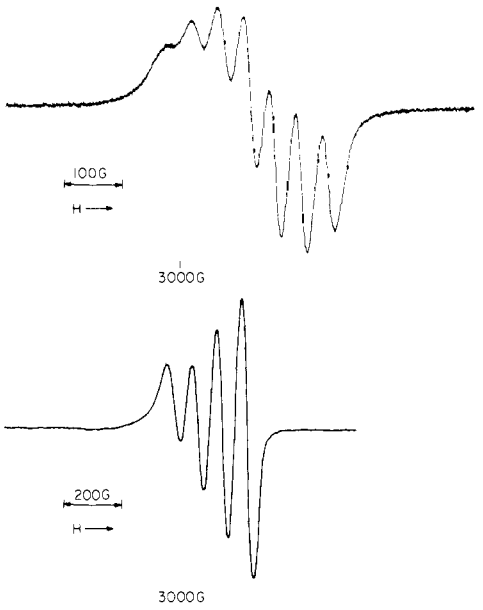

Figure 5. Ambient temperature EPR spectra of $Cu^{II}Cu^{I}L(ClO_4)$ dissolved in CH_2Cl_2 under helium (top) and CO (bottom) atmospheres. Note that different field scales are used.

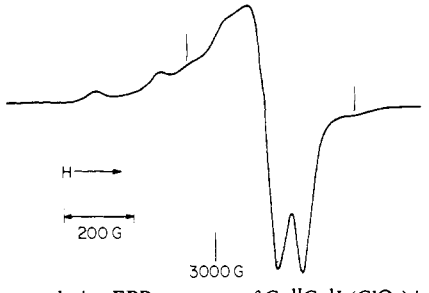

Figure 6. Frozen solution EPR spectrum of $Cu^{II}Cu^{I}L(ClO_4)$ in acetonitrile at 77 K. The two vertical lines indicate contributions from the triplet spectrum arising from dimerization. See ref 17.

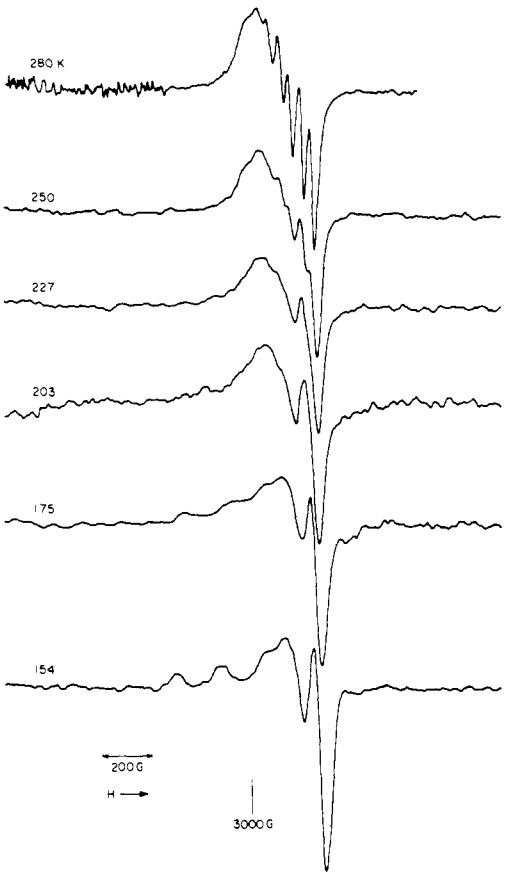

Figure 7. Variable-temperature EPR spectra of $Cu^{II}Cu^{I}L(ClO_4)$ dissolved in CH_2Cl_2/toluene (3/2 by volume).

at half that for $Cu^{II}Cu^{I}LCO^{+}$ ($A_7 = 1/2A_4$) is predicted on theoretical grounds.[16] No hyperfine structure attributable to nitrogen has been seen in these spectra.

The solid-state spectra of $Cu^{II}Cu^{I}L(ClO_4)$ and $Cu^{II}Cu^{I}L(CO)ClO_4$ exhibit a single symmetrical line at both low and ambient temperatures with very similar values. The lack of any resolution is likely due to dipolar line broadening.

Spectral studies in frozen media met with several experimental complications. The anisotropic spectrum of $Cu^{II}Cu^{I}L(CO)ClO_4$ in frozen CH_2Cl_2 (solutions of $Cu^{II}Cu^{I}L(ClO_4)$ exposed to CO before freezing) is straightforward, consisting of a four-line pattern for $g_{\parallel}$ with $g_{\perp}$ not resolved. Frozen solutions of $Cu^{II}Cu^{I}L(ClO_4)$ in CH_3CN or CH_3CN/toluene (1:1), the latter combination forming good glasses, give essentially the same spectra as for $Cu^{II}Cu^{I}L(CO)ClO_4$ yet the spectra are often accompanied by additional features (Figure 6) whose intensities decrease relative to the main lines as temperature increases and concentration decreases. That the extra features are likely due to dimer formation is supported by the observation in a CH_3CH_2OH/CH_3OH (4/1) glass of a spectrum characteristic of a spin triplet.[17] Another complication which occasionally occurred in experiments with frozen solutions of $Cu^{II}Cu^{I}L(ClO_4)$ in CH_2Cl_2 was the observation of broad bands presumably due to precipitated solid.

In spite of these experimental difficulties the principal observation was the change from the seven-line spectrum for $Cu^{II}Cu^{I}L(ClO_4)$ at room temperature to a four-line pattern at liquid nitrogen temperature, or lower, in contrast to the apparent localized behavior of $Cu^{II}Cu^{I}L(CO)ClO_4$ on the EPR time scale at both temperatures. Consequently, spectra of $Cu^{II}Cu^{I}L(ClO_4)$ in CH_2Cl_2 were recorded at various temperatures to determine if a transition temperature range could be located. The results obtained in a CH_2Cl_2/toluene (3:2) mixture are presented in Figure 7. Spectra were obtained from 84 K (distinct anisotropic four-line spectrum) to 280 K (seven lines, well resolved) although a more limited range is indicated in the figure. To alleviate dimerization and precipitation problems dilute solutions were used, giving less than optimum resolution. Nevertheless, the gross aspects are readily evident. At 154 K the anisotropic spectrum indicative of a localized electron can be seen. At 175 K the low-field $g_{\parallel}$ lines have converged somewhat on the central lines. In the 203–227 K range all lines have clearly coalesced. At 250 and 280 K new features arise, due to the hyperfine interaction involving two copper centers. The observation of an anisotropic four-line pattern rather than an isotropic spectrum near the coalescence region where the solution is probably fluid may be due to a slow rate of molecular tumbling, such that directional characteristics are not averaged on the EPR times scale.

Under most conditions the spin doublet spectra of frozen solutions of $Cu^{II}Cu^{I}L(ClO_4)$ have displayed no structure which might be assigned to hyperfine coupling to nitrogen. Dilute CH_2Cl_2 solutions have, however, occasionally shown such splitting (~15 G) in the $g_{\perp}$ line.

Magnetic Susceptibility. Room temperature magnetic susceptibilities are reported in Table IV. The values for the magnetic moments for $Cu^{II}Cu^{I}L(ClO_4)$ (1.81 μ_B) and $Cu^{II}Cu^{I}L(CO)ClO_4$ (1.94 μ_B) are typical of magnetically dilute Cu^{II} complexes. These results contrast with the μ_{eff} for $Cu^{II}Cu^{II}L(ClO_4)_2 \cdot 2H_2O$ (0.60 μ_B), which indicates quite strong coupling between the Cu^{II} centers in agreement with

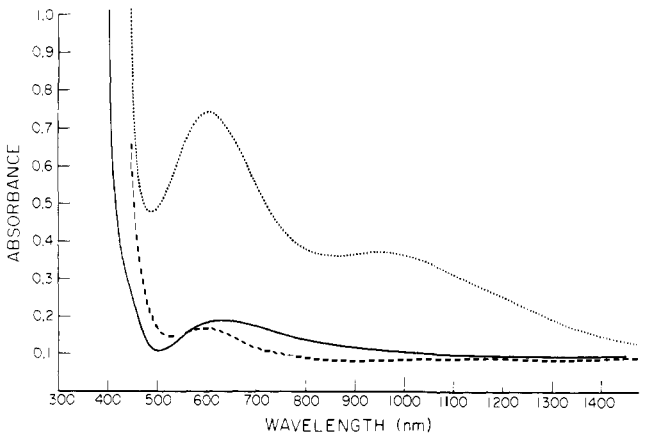

Figure 8. Electronic absorption spectra in methanol of $Cu^{II}Cu^{II}L(ClO_4)_2 \cdot 2H_2O$ (1.15×10^{-3} M), – –; $Cu^{II}Cu^{I}L(ClO_4)$ (1.10×10^{-3} M) under helium, ·····; $Cu^{II}Cu^{I}L(CO)ClO_4$ (1.10×10^{-3} M) under carbon monoxide, – – –.

Table IV. Magnetic Moments at 25 °C

compd	μ_{eff}, μ_B
$Cu^{II}Cu^{II}L(ClO_4)_2 \cdot 2H_2O$	0.60 ± 0.04
$Cu^{II}Cu^{I}L(ClO_4)$	1.81 ± 0.04
$Cu^{II}Cu^{I}L(CO)(ClO_4)$	1.94 ± 0.04
$Cu^{I}Cu^{I}L$	0.19 ± 0.25
$Zn^{II}Zn^{II}L(ClO_4)_2 \cdot 2H_2O$	0.00 ± 0.25

Robson's observations.[2] As expected, $Zn^{II}Zn^{II}L(ClO_4)_2 \cdot 2H_2O$ and $Cu^{I}Cu^{I}L$ are diamagnetic, within experimental error.

Electronic Absorption Spectra. Some aspects of the electronic absorption spectra essential to the characterization of $Cu^{II}Cu^{I}L(ClO_4)$ as a mixed-valence species were reported earlier.[5] Representative spectra of $Cu^{II}Cu^{II}L(ClO_4)_2 \cdot 2H_2O$, $Cu^{II}Cu^{I}L(ClO_4)$, and $Cu^{II}Cu^{I}L(CO)ClO_4$ ($Cu^{II}Cu^{I}L^+$ exposed to CO) in methanol in the visible and near-infrared regions are shown in Figure 8. All three spectra exhibit the tail of an intense absorption in the ultraviolet region with band maxima in the range 350-400 nm ($\epsilon \sim 10\,000\ M^{-1}\ cm^{-1}$). This band occurs in the yellow complex $Zn^{II}Zn^{II}L(ClO_4)_2 \cdot 2H_2O$ and is presumably due to an intraligand transition. Some charge-transfer character undoubtedly is present in the copper complexes. A band of considerably greater intensity is evident at ~250 nm; it is probably of $\pi \rightarrow \pi^*$ origin. In the visible region $Cu^{II}Cu^{II}L^{2+}$ (green) displays a much weaker asymmetric band which does not occur in the dizinc complexes, with a maximum at 600 nm (ϵ 85 in CH_3CN) and a shoulder at 700 nm (ϵ 60 in CH_3CN) in agreement with Robson's observations and presumably due to ligand-field transitions.[2]

Solutions of $Cu^{II}Cu^{I}L(ClO_4)$ were reported to exhibit a very broad band in the near-IR region in certain solvents, which was attributed to an intervalence transfer (IT) transition

$$Cu^{II}Cu^{I} \xrightarrow{h\nu} Cu^{I}Cu^{II}*$$

(the product in a vibrationally excited state) in addition to an appreciable enhancement of the 600-nm band.[5] The position of the IT band appeared to be solvent dependent; it occurred at 1200 nm in noncoordinating CH_2Cl_2 and at 900-1000 nm in the weakly coordinating solvents CH_3OH, $(CH_3)_2CO$, and DMF, while no such band was apparent in CH_3CN, which has a strong affinity for Cu^{I}. Initial spectra were recorded to 1700 nm[5] but the spectral range has now been extended to 2600 nm. The spectrum of $Cu^{II}Cu^{I}L(ClO_4)$ in CH_2Cl_2 out to this limit is shown in Figure 9, where an additional band can be seen at 1700 nm. Thus, earlier spectra terminated on the plateau of

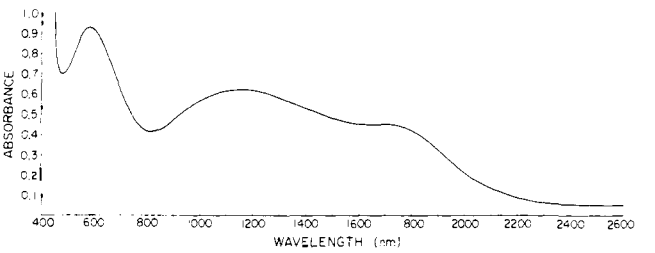

Figure 9. Electronic absorption spectrum of $Cu^{II}Cu^{I}L(ClO_4)$ (0.822×10^{-3} M) in dichloromethane under helium.

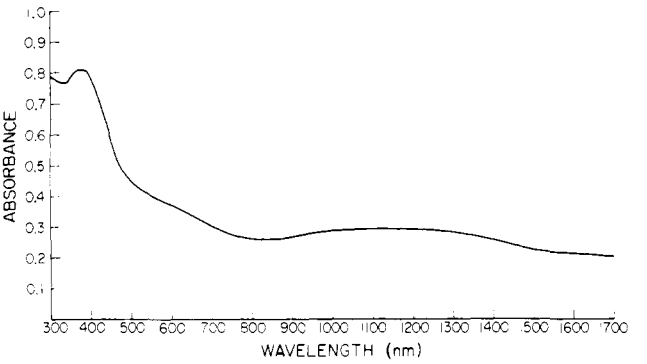

Figure 10. Electronic absorption spectrum of $Cu^{II}Cu^{I}L(ClO_4)$ in a Nujol mull.

the new band maximum rather than at the true base line, and the higher energy bands (600 and 1200 nm) are actually much more intense than initially believed. Similar reinvestigation in CH_3OH was complicated by solvent vibrational overtone bands which partially obscure any broad features in the 1700-nm region. Hence it is not clear whether such a band is present in the CH_3OH spectra. In contrast to the bluish-green color of $Cu^{II}Cu^{I}L(ClO_4)$ in non- or weakly coordinating solvents, CH_3CN solutions are brown because the UV band (λ_{max} 380 nm), which is much broader in this solvent than in CH_2Cl_2, tails off farther into the visible to overlap with the 600-nm band. Acetonitrile solutions revealed no feature in the near-IR region of intensity comparable to that seen in the spectra of the other solutions. All solutions of $Cu^{II}Cu^{I}L(ClO_4)$ turn green rapidly on exposure to oxygen and show only a weak ligand field absorption (λ_{max} ~650 nm) in the visible and near-IR regions. This observation is consistent with the assignment of the IR bands as intervalence transitions.

As expected from its dark brown color in the solid state, mull spectra of $Cu^{II}Cu^{I}L(ClO_4)$, Figure 10, shows that the near-UV band tails into the visible to overlap the 600-nm absorption. Also, this spectrum clearly exhibits a very broad band in the near IR. Figure 11 shows a very concentrated mull spectrum on a more compressed wavelength scale and farther into the IR. A band at 1800 nm is clearly resolved while another at 1300 nm is accompanied by a shoulder at 1050 nm. Over a period of days (3-5) the mulls turn green in laboratory atmosphere, and again only a weak band due to Cu^{II} is observed in the spectra at wavelengths greater than 500 nm.

Since the EPR results demonstrate that dimerization of $Cu^{II}Cu^{I}L^+$ occurs in frozen solution under certain conditions, the question arose whether the "IT" bands could result from intermolecular interaction in fluid solution, especially in CH_3OH. Beer's law studies were conducted for CH_3OH solutions (600- and 900-nm bands) and CH_2Cl_2 solutions (600-, 1200-, and 1700-nm bands) over a 50-fold concentration change (10^{-3} to 2×10^{-5} M) at the ambient temperature. For all bands examined the dependence of absorbance on concentration was strictly linear. The lack of any deviation from Beer's law behavior suggests that there is no change in the

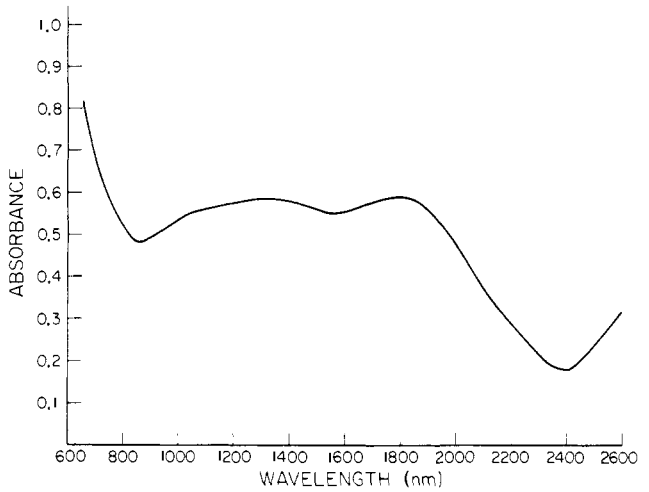

Figure 11. Electronic absorption spectrum of $Cu^{II}Cu^{I}L(ClO_4)$ in a Nujol mull (more concentrated mull than in Figure 10).

absorbing species in the concentration range employed. This Beer's law behavior, in light of the observed seven-line isotropic EPR spectrum obtained for $Cu^{II}Cu^{I}L^{+}$ in CH_3OH at 25 °C, suggests that the IR bands are attributable to a monomeric binuclear species. Electronic absorption spectral data for $Cu^{II}Cu^{I}L(ClO_4)$ are summarized in Table V.

Exposing $Cu^{II}Cu^{I}L^{+}$ in any of the solvents discussed to CO generates yellow solutions of the carbonyl adduct. The spectrum in CH_3OH is shown in Figure 8. It displays only a single weak band ($\epsilon \sim 80$ in CH_3OH) at 600 nm (λ_{max} varies slightly in different solvents) which is probably due to a ligand-field transition. Significantly the broad IR bands and the enhanced intensity of the 600-nm band observed for solutions of $Cu^{II}Cu^{I}L(ClO_4)$ have disappeared.

It is notable that the $Cu^{II}Cu^{I}$-acetate system in methanol also exhibits more than one band in the visible-near-IR portion of its spectrum. A sharp band at 509 nm and a broad band centered at 900 nm were reported. The precursor complexes, $Cu^{I}(CH_3CN)_4^{+}$ and $Cu^{II}(H_2O)_6^{2+}$, are essentially transparent at these wavelengths.[15]

$Cu^{I}Cu^{I}$ Compounds. The very low solubility of $Cu^{I}Cu^{I}L$ limited attempts to obtain solution electronic spectra of this compound. Saturated solutions in DMF showed only a band at 380 nm which tailed into the visible region with no absorption above 700 nm. Mull spectra of this complex also contained the 380-nm band, a shoulder at 475 nm, and an extremely long tail which extended out to 1500 nm. Solution spectra of $Cu^{I}Cu^{I}L(CO)_2$ contained only an intense band at 410 nm and a prominent shoulder at 600 nm.

Discussion

Electrochemistry. Given the experimental data presented herein for $Cu^{II}Cu^{I}L(ClO_4)$ and $Cu^{I}Cu^{I}L$, along with the fact that $Zn^{II}Zn^{II}L^{2+}$ has no observable electrochemistry, it is clear that both electrochemical waves found for $Cu^{II}Cu^{II}L^{2+}$ are due to the reduction of Cu^{II} to Cu^{I}. Reduction of the two Cu^{II} atoms in $Cu^{II}Cu^{II}L^{2+}$ can be discussed either by treating each site separately or by viewing both atoms and the macrocyclic ligand as a unit. The former method is more useful for comparing the reduction potentials to other monomeric systems, while the latter method is more suitable for comparisons with other multimetal systems.

As judged by the formal reduction potentials E_1^f and E_2^f, both Cu^{I} centers in $Cu^{I}Cu^{I}L$ are strongly reducing. In fact, the data in Tables I and II indicate that $Cu^{I}Cu^{I}L$ is a stronger reducing agent than superoxide ion. Since the E^0 for the reduction of Cu^{II} to Cu^{I} in water is +0.153 V,[21] it appears that

Table V. Electronic Absorption Spectral Data for $Cu^{II}Cu^{I}L(ClO_4)$

medium	λ_{max}, nm ($\sim\epsilon$)
solid	600 sh, 1050, 1300, 1800,
CH_2Cl_2	580 (980), 1175 (640), 1725 (430)
CH_3OH	605 (930), 975 (430)
DMF	600 (920), 950 (420)
$(CH_3)_2CO$	600 (920), 1000 (480)
CH_3CN	600

the binucleating ligand, L, stabilizes Cu^{II} much more than it stabilizes Cu^{I}. Although anionic oxygen ligands would be expected to favor Cu^{II} over Cu^{I}, unsaturated nitrogen donors can have the opposite effect. For example, the reduction of Cu^{II} to Cu^{I} in acetonitrile occurs at $\sim$+0.95 V.[22] The nearly square-planar coordination geometry enforced by the ligand[23] is probably the overriding reason that Cu^{II} is stabilized over Cu^{I}, because the latter prefers a tetrahedral environment. Since reduction of the copper atoms in $Cu^{II}Cu^{II}L^{2+}$ to Cu^0 was not observed electrochemically, it is not clear whether the observed solution stability of $Cu^{II}Cu^{I}L^{+}$ and $Cu^{I}Cu^{I}L$ toward disproportionation to copper metal is thermodynamic or merely kinetic.

One might expect E_1^f and E_2^f to be similar to the $E_{1/2}$ value of Cu(saltn), −1.099 V, assuming coordination geometries to be similar and ignoring the effects of one copper atom on the other. The observed differences are probably due to molecular charge. The dicationic $Cu^{II}Cu^{II}L^{2+}$ and cationic $Cu^{II}Cu^{I}L^{+}$ are respectively 0.58 and 0.19 V easier to reduce than the neutral Cu^{II}(saltn). A more meaningful comparison can be made between E_1^f and the reduction of $Cu^{II}Zn^{II}L^{2+}$ which occurs at −0.628 V.[24] Note that the $Cu^{II}Cu^{II}$ complex is $\sim$0.1 V easier to reduce than $Cu^{II}Zn^{II}$ complex. A similar situation is found for $[(NH_3)_5Ru^{III}(pyr)Ru^{III}(NH_3)_5]^{6+}$, which is 0.05 V easier to reduce than its best "monomer", $[(NH_3)_5Ru^{III}(pyr)Rh^{III}(NH_3)_5]^{6+}$.[25]

Recently, Patterson and Holm[26] compared the reduction potentials of a series of neutral Cu^{II} chelates with potentials for "blue" copper sites in proteins. As with the majority of the neutral chelates, the potentials reported in this paper for $Cu^{II}Cu^{II}L^{2+}$ are at least 1.0 V more cathodic than the "blue" copper sites, which occur at $\sim$0.5 V. Likewise, the redox potentials for $Cu^{II}Cu^{II}L^{2+}$ are considerably more reducing than are those for type III copper sites.[27,28] Although type III copper sites and $Cu^{II}Cu^{II}L(ClO_4)_2 \cdot 2H_2O$ both contain a pair of magnetically coupled copper atoms,[2,29] differences in redox potentials argue that ligand environments in the two cases are quite different.

Molecules that contain two or more chemically equivalent and reversible redox sites exhibit electrochemistry which is dictated by the thermodynamic relationships between various molecular redox states. This subject has been examined in the literature both theoretically and experimentally.[30-34] For the case of a molecule with two sites, reduction potentials and the conproportionation constant, K_{con}, are related in the following way:

$$\text{Ox-Ox} + e^- \overset{E_1^f}{\rightleftharpoons} \text{Ox-Red}$$

$$\text{Ox-Red} + e^- \overset{E_2^f}{\rightleftharpoons} \text{Red-Red}$$

$$\text{Ox-Ox} + \text{Red-Red} \overset{K_{con}}{\rightleftharpoons} 2(\text{Ox-Red})$$

$$E_1^f - E_2^f = 0.0591 \log K_{con}$$

It is natural to divide the two-site case into three classes based on the value of K_{con}.

$K_{con} = 4$. This is the totally noninteracting case, i.e., the oxidation state of one site is not affected by the oxidation state of the other. Even though the two sites have the same microscopic redox potentials, notice that E_1^f and E_2^f, which are macroscopic properties, are not equal but are separated by 0.0356 V. This separation is due to statistics and has been observed for certain polyferrocenes.[33,35]

$K_{con} < 4$. This implies that the second electron is easier to add than the first, $E_1^f - E_2^f < 0.0356$ V, and that the mixed-valence molecule, Ox-Red, will be unstable with respect to disproportionation. If both sites in the molecule do not change geometrically or chemically, it is unlikely that this case will occur because charge should be sequentially more difficult to add. In situations where this case does occur, addition of the first electron is usually followed by some process such as bond breaking,[36] rotation about a bond,[34] or protonation.[37] The process causes the second site to be easier to reduce than the first.

$K > 4$. In this case the second electron is more difficult to add than the first, $E_1^f - E_2^f > 0.0356$ V, and Ox-Red is stable. This situation is the most common and is observed, for example, in many ruthenium dimers,[38] certain biferrocenes,[35] and $Cu^{II}Cu^{II}L(ClO_4)_2 \cdot 2H_2O$.

The observation that $Cu^{II}Cu^{II}L^{2+}$ does reduce in two sequential, one-electron steps appears to be in conflict with other electrochemical studies on oxo-bridged, binuclear copper systems. The binuclear complex $Cu^{II}Cu^{II}([PAA)_2en]$ (drawn below) was reported to reduce in one reversible two-electron step.[42] This result is especially unusual considering the difference in ligands for the two coppers. Indeed we have examined $Cu^{II}Cu^{II}([PAA)_2en]$ in our laboratory by dc polarography and constant-potential electrolysis and find that it reduces in a single reversible *one*-electron process.[43] More recently, Lintvedt reported that the two copper atoms in $Cu^{II}Cu^{II}(BAA)_2$ (drawn below) reduce at exactly the same potential.[44] The conclusion that $E_1^f = E_2^f$ for $Cu^{II}Cu^{II}(BAA)_2$ does not mean that the two centers reduce with equal ease, because this molecule belongs to the $K < 4$ class and the second electron is microscopically easier to add than the first. The two-electron reduction at a single potential may result from a conformational change accompanying the first one-electron reduction which facilitates the second one-electron process. The electrochemistry for $Cu^{II}Cu^{II}L^{2+}$ is quite consistent with results on a similar system, $Cu^{II}Cu^{II}L'^{2+}$ (drawn below), reported by Addison, in that the molecule is reduced in two one-electron steps.[45]

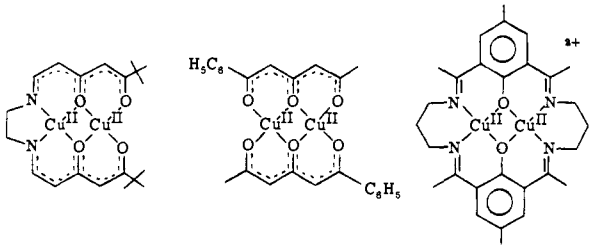

Cu(II)Cu(II)[(PAA)$_2$en] Cu(II)Cu(II)(BAA)$_2$ Cu(II)Cu(II)L'$^{2+}$

Properties of the Mixed-Valence Complexes. Our studies of the mixed-valence characteristics of $Cu^{II}Cu^{I}L(ClO_4)$ and $Cu^{II}Cu^{I}L(CO)ClO_4$ were concerned with their description in terms of existing models. We were especially interested in qualitatively gauging the extent of interaction between the metal centers in the ground state, i.e., are these species better represented as $Cu^{II}Cu^{I}$ or $Cu^{1.5}Cu^{1.5}$? Were the former description appropriate, we hoped to obtain an estimate of the rate of thermal transfer of the odd electron between the two metal sites. Mixed-valence materials often exhibit spectral behavior and other physical properties not shown by the isolated ions; in particular, the intervalence transfer (IT) transition represents a photoinduced electron transfer from one metal atom to the other. Robin and Day developed a classification scheme of mixed-valence systems based on amount of delocalization of the odd electron between metal centers in the ground electronic state.[46] At the same time Hush proposed a coupled harmonic oscillator model for weakly interacting systems which relates the energy of the optical electron transfer (E_{op}) to that of the corresponding thermal activation barrier (E_{th}).[47] For a symmetric complex this relation is $E_{op} = 4E_{th}$. From E_{th} it is possible to calculate a rate constant for the radiationless transfer. Criteria exist for assessing the validity of linking E_{th} to E_{op} in this fashion. These include, principally, agreement between the observed IT spectral bandwidth and that calculated from the model and a solvent dependence of E_{op} such that the media behave as dielectric continua. The latter restriction arises because E_{op} represents the inner- and outer-sphere reorganizational energies ($E_{op} = \lambda_i + \lambda_o$) in the Hush model. A number of complexes have met these criteria.[48,49] The application of this model has been challenged for other systems, however, particularly when the calculated rate is at variance with an experimentally determined value such as for biferrocenium $(Fe^{II}Fe^{III})^+$.[50,51] The complex $(NH_3)_5Ru(pyr)Ru(NH_3)_5^{5+}$ does not meet either of the spectral tests given above, yet conflicting results from a variety of physical measurements have been reported regarding its definitive classification and corresponding k_{th}.[25,52,53]

The mixed-valence copper complexes reported here can be discussed within this context. For the CO complex the observation of a localized odd electron at both high and low temperatures indicates that thermal electron transfer either is prevented entirely or is too slow to be observed on the EPR time scale at either temperature. This is consistent with the lack of any band in the visible-near-IR region of the electronic spectrum assignable to an IT transition. It might, however, occur at higher energy obscured by the high-intensity bands of the UV region. The binding of CO to the Cu^{I} site would be expected to markedly alter the energy differences between Cu^{I} and Cu^{II} perhaps to an extent which makes facile electron transfer infeasible. Based on its spectral properties $Cu^{II}Cu^{I}L(CO)ClO_4$ behaves as though it contains noninteracting metal centers—a class I species.

The magnitude of K_{con} for $Cu^{II}Cu^{I}L^+$ (4.83×10^6) can be compared to values for several well-characterized, symmetric ruthenium systems. The mixed-valence ions $[(NH_3)_5Ru(4,4'\text{-bpy})Ru(NH_3)_5]^{5+}$ and $[Cl(bpy)_2Ru(pyr)Ru(bpy)_2Cl]^{3+}$ (bpy = 2,2-bipyridine) are class II systems which obey the Hush model.[39] The values of K_{con} for these compounds are 4–20[40] and 300,[39] respectively. When similar ruthenium systems are oxo bridged two delocalized class III ions can be formed, $[Cl(bpy)_2RuORu(bpy)_2Cl]^{3+}$ and $[Cl(bpy)_2RuORu(bpy)_2Cl]^+$, with K_{con} equal to 6.49×10^{20} and 3.2×10^{11}.[41] Controversy still exists as to the classification of the ion $(NH_3)_5Ru(pyr)Ru(NH_3)_5^{5+}$. Meyer has noted, however, that the value of K_{con} in this system, 1.89×10^7, is much larger than in the weakly interacting class II systems.[39] Electrochemical measurements on $Cu^{II}Cu^{I}L^+$ thus indicate a fairly strong interaction but no clear indication as to whether it should be regarded as a class II or class III ion.

The complex $Cu^{II}Cu^{I}L(ClO_4)$ also displays evidence of interaction between Cu^{I} and Cu^{II} in its electronic and EPR spectra. The room temperature EPR spectra can best be interpreted in terms of intramolecular electron transfer between coppers at a rate which is rapid compared to the relatively slow resonance experiment. In frozen media (solutions where dimerization is not a problem) that exchange is stopped or is too slow to be monitored. The variable-temperature experiments reveal that coalescence takes place at about 200 K, which is probably well above the freezing point of a CH_2Cl_2/toluene

solution of the complex. Hence, the inhibition of electron exchange is not a consequence of solution freezing. A number of explanations are conceivable for this behavior. First, axial ligation by ClO_4^- or solvent at lower temperatures might lead to an asymmetric complex similar to $Cu^{II}Cu^{I}L(CO)^+$. Solvent coordination seems likely for CH_3CN but unlikely for CH_2Cl_2, which was utilized for many of the spectroscopic studies. Another cause might be that at the lower temperatures insufficient thermal energy is available to effect macrocyclic conformational changes necessary for the radiationless transfer. According to the accepted picture of thermal electron exchange, geometrical adjustments (bond-length changes in simple molecules) to equalize the environments of both metal sites occur prior to electron migration.[54] For $Cu^{II}Cu^{I}L^+$ this might involve a structure intermediate between square planar for Cu^{II} and square planar with slight tetrahedral distortion for Cu^{I}. The molecular structure of a macrocyclic mononuclear Cu^{I} complex which is essentially square planar about copper but exhibits a perceptible tetrahedral twist was recently determined in this laboratory.[55] Such a molecular deformation in solution should require considerably more energy than in simpler systems, e.g., self-exchange between mononuclear octahedral complexes, and the different coordination geometries for Cu^{I} and Cu^{II} might be interconvertible at a very slow rate (if at all) at low temperature. Support for the latter interpretation comes from Addison's results on the analogous $Cu^{II}Cu^{I}$ complex with methyl groups on the imine carbon atoms, $Cu^{II}Cu^{I}L'^+$ (see drawing of $Cu^{II}Cu^{I}L'^{2+}$ earlier in this paper).[45] The ambient-temperature EPR spectrum for this species, $Cu^{II}Cu^{I}L'^+$, displays only four hyperfine lines suggesting that the odd electron is localized on one copper atom. The larger methyl substituents may effectively hinder the requisite conformational changes for an EPR-detectable exchange process. Our data do not favor one explanation over the other; indeed both processes may occur. In any event the EPR results are not sufficient to distinguish $Cu^{II}Cu^{I}L(ClO_4)$ as a class II or class III mixed-valence system.

The variable-temperature spectra permit an estimate of the rate of electron exchange. If k_{th} is taken to be roughly equal to the EPR lifetime ($5.5 \times 10^8\ s^{-1}$)[56] at the coalescence temperature (~200 K), then a value for $E_{th}^{\ddagger}$ can be obtained using the relation

$$k_{th} = \frac{kT}{h} e^{-E_{th}^{\ddagger}/RT}$$

where the symbols have their usual meaning from absolute reaction rate theory, and the transmission coefficient is assumed to be unity for adiabatic electron transfer.[48] This gives a value of 3.5 kcal for the activation barrier and assuming the same value at room temperature yields $1.7 \times 10^{10}\ s^{-1}$ for k_{th} at 298 K. It is to be emphasized that these calculations are merely a rough approximation and are contingent upon the validity of the frequency term and the assumption that no mechanistic change occurs between 200 and 298 K.

Other mixed-valence systems have been reported to show temperature dependence in their thermal electron transfer properties. For example, in a Mössbauer study the spectra of a series of trinuclear iron clusters $Fe^{II}Fe^{III}{}_2O(CH_3CO_2)_6 \cdot L_x$ were recorded at several temperatures (77–298 K) and the iron valences became indistinguishable on this time scale ($10^7\ s^{-1}$).[57]

The electronic spectra of $Cu^{II}Cu^{I}L(ClO_4)$ in various media are complicated, and definitive interpretation is not possible at present. That the bands in the near-IR and visible regions are due primarily to intervalence transfer is consistent with the disappearance of the IR bands and the intensity reduction of the 600-nm bands on exposure to CO or O_2 and the lack of these features in the $Cu^{II}Cu^{II}$ and $Cu^{I}Cu^{I}$ complexes, although the low solubility of $Cu^{I}Cu^{I}L$ made it impossible to obtain spectra of solutions of comparable concentration. The intensities of these absorptions are large enough to preclude their assignments as pure ligand-field transitions even for low-symmetry environments. Their relatively low energies make them unlikely candidates for charge transfer involving ligands (N and O donors in this macrocycle).

Application of the Hush model to relate the thermal and optical electron transfer processes in a simple fashion is probably inappropriate in this system. For copper complexes the solvent molecules can be regarded as more or less directly involved, depending on their donor strength, in the inner coordination sphere of either or both oxidation states. This would influence the energy of both the thermal and photoinduced processes in a manner different from the effect of a dielectric continuum. Moreover, the varying number of bands observed complicates the use of a simple model. In addition to the basic IT transition involving the same d orbitals on different metal atoms, transitions to empty higher energy orbitals or from filled lower energy d orbitals are possible. These additional bands should occur at energies roughly corresponding to the IT transition plus an associated ligand-field transition. Such bands have been reported for Prussian blue $KFe^{II}Fe^{III}(CN)_6 \cdot H_2O$[58] and biferrocenium $(Fe^{II}Fe^{III})^+$.[51] For $Cu^{II}Cu^{I}L(ClO_4)$ a similar interpretation of the spectra might hold. The variation in the number of bands observed with different solvents and in the solid state is reminiscent of the behavior of the ligand-field spectra of certain square-planar Cu^{II} complexes, notably $Cu(acac)_2$ toward solvents of different donor strength.[59] Yet no orbital energy ordering for square-planar or square-pyramidal geometries can satisfactorily account for the solvent independence of the 600-nm band. A less speculative discussion of the electronic spectra of this complex will require additional research.

$Cu^{I}Cu^{I}$ Compounds. All of the physical studies on $Cu^{I}Cu^{I}L$ (elemental analysis, IR spectroscopy, and magnetic susceptability) are consistent with its formulation as a $Cu^{I}Cu^{I}$ compound. Relatively few binuclear $Cu^{I}Cu^{I}$ compounds are known, although recently attempts to model binuclear copper sites in proteins have led to the synthesis of several such compounds.[60-63] The lack of solubility for this compound has precluded extensive characterization in solution. On the other hand, since $Cu^{I}Cu^{I}L(CO)_2$ could not be isolated from solution, the evidence for its existence consists of the stoichiometry involved in its preparation and the CO stretching band in the solution IR spectrum. Further study is obviously required for these systems.

Conclusion

Use of a binucleating macrocyclic ligand has led to isolation of mixed valence, $Cu^{II}Cu^{I}$, and fully reduced, $Cu^{I}Cu^{I}$, complexes in which each copper ion experiences a similar coordination environment. The mixed-valence species $Cu^{II}Cu^{I}L^+$ exhibits unusual electronic absorption and temperature-dependent EPR spectral properties. The latter permit an estimate of $1.7 \times 10^{10}\ s^{-1}$ for the rate of thermal intramolecular electron transfer. Both $Cu^{II}Cu^{I}L^+$ and $Cu^{I}Cu^{I}L$ reversibly bind CO forming $Cu^{II}Cu^{I}L(CO)^+$ and $Cu^{I}Cu^{I}L(CO)_2$, respectively, new examples of five coordination for Cu^{I}.

Experimental Section

Materials. All chemicals were reagent grade and were used as received unless otherwise noted. Copper(II) perchlorate, ground to a powder, then dried to a constant weight in vacuo (25 °C), was used as $Cu(ClO_4)_2 \cdot 6H_2O$. Tetrabutylammonium perchlorate TBAP (Southwestern Analytical Chemicals) was dried exhaustively in vacuo (25 °C) before use. Reagent grade *N,N*-dimethylformamide (DMF) was dried successively over $MgSO_4$ and $CuSO_4$ and then over 4A molecular sieves for 48 h and vacuum distilled. 5-Methyl-2-hydroxyisophthalaldehyde was prepared by a modification of the literature method.[64]

Physical Measurements. Sample preparation for physical studies on the air-sensitive materials were accomplished in a Vacuum Atmospheres Dri-lab glovebox with a helium atmosphere. Thoroughly deaerated spectroquality solvents were used for solution studies.

Magnetic susceptibility determinations were done with powdered samples at room temperature using a Cahn Instruments Faraday balance. $HgCo(SCN)_4$ was used as a calibrant, and diamagnetic corrections were made using Pascal's constants.

X-Band EPR spectra were recorded on a Varian E-line spectrometer. Temperature control was achieved with an Air Products Heli-Tran liquid helium transfer refrigerator. Samples were contained in cylindrical quartz tubes of 2- or 3-mm diameter equipped with stopcocks and ⅌ 14/20 joints. Solutions of the carbonyl complex, $Cu^{II}Cu^{I}L(CO)^{+}$, were generated from those of $Cu^{II}Cu^{I}L^{+}$ by evacuating the helium atmosphere in the cell and then admitting carbon monoxide gas.

Electronic spectra were recorded on Cary 14 spectrophotometers. Solid-state spectra were obtained with Nujol mulls on filter paper with the mulling agent in the reference compartment. Solution spectra were recorded using 1-cm quartz cells equipped with stopcocks to facilitate addition of CO as described for the EPR procedure. Solvent was run against solvent to obtain a base line.

Infrared spectra were recorded on a Beckman IR-12 infrared spectrophotometer. Solid-state spectra were recorded using Nujol mulls pressed between KBr plates. Solution spectra were obtained using calcium fluoride solution cells (1 mm).

Carbon monoxide stoichiometries were obtained using a modified Warburg manometer. Both the cell and buret system were water jacketed at 22 °C. The uptakes were performed at a constant pressure of 741 mmHg.

Electrochemistry. The apparatus used for constant-potential electrolysis (CPE) and cyclic voltammetry consisted of a Princeton Applied Research Model 173 potentiostat-galvanostat coupled with a Model 179 digital coulometer, plus a voltage ramp generator of our own design. A PAR Model 174A polarographic analyzer was used for dc polarography and differential pulse voltammetry. For display purposes, both a storage oscilloscope and a X-Y recorder were used.

Constant-potential electrolysis and cyclic voltammetry were done in a three-compartment H cell. The cell consisted of 25-mL working and auxiliary compartments separated by a small center compartment, all separated by medium-porosity sintered glass frits. In all solvents the supporting electrolyte was 0.1 M TBAP.[6] For CPE the working electrode was a mercury pool and for every technique the auxiliary electrode was a coiled platinum wire. The reference electrode consisted of a silver wire immersed in an acetonitrile solution containing $AgNO_3$ (0.01 M) and TBAP (0.1 M), all contained in a 9-mm glass tube fitted on the bottom with a fine porosity sintered glass frit.

All potentials are reported vs. the normal hydrogen electrode (NHE). Instead of attempting to correct potentials measured against the $Ag/AgNO_3$ (0.01 M), TBAP (0.1 M), CH_3CN reference electrode, an internal reference redox couple was used. It has been proposed that the oxidation of ferrocene to ferrocenium ion occurs at the same potential in every solvent.[65] In water the process occurs at +0.400 V vs. NHE.[66] Experimentally, small amounts (5×10^{-5} to 10^{-3} M) of ferrocene were added to solutions containing the compounds of interest and formal potentials for both couples were measured under the same conditions. Ferrocene is not easily reduced and did not react with the reduced forms of the copper complexes. Comparison of potentials to ferrocene oxidation is more reproducible and provides a better estimate of potentials vs. the NHE because unknown junction potentials associated with the Ag/Ag^{+} or saturated calomel electrodes are avoided.

$Cu^{II}Cu^{II}L(ClO_4)\cdot 2H_2O$ was prepared via a modification of the method reported by Robson.[2] 1,3-Diaminopropane (1.19 g, 1.34 mL, 16 mmol) was slowly added to a solution of $Cu(ClO_4)_2\cdot 6H_2O$ (5.9 g, 16 mmol) in methanol (25 mL). A second solution containing 5-methyl-2-hydroxyisophthalaldehyde (2.5 g, 15.2 mmol) in boiling methanol was then added dropwide to the copper-amine mixture. The resulting solution was heated to boiling for 1 h and cooled to room temperature. The solution was reduced to a small volume (~20 mL) using a rotary evaporator and was cooled for several hours in a refrigerator. A light green solid formed which was removed by filtration. The filtrate was further reduced in volume by evaporation until just before dryness. During this process more solid formed which was collected and combined with the original precipitate. After being washed with cold water and air dried, the solid was added to boiling water (~100 mL/g of solid), stirred for about 5 min, and filtered. Slow cooling of the filtrate yielded emerald-green needles which were isolated by vacuum filtration, washed with cold water, and dried under vacuum. Anal. Calcd for $C_{24}H_{30}N_4O_{10}Cl_2Cu_2$: C, 37.71; H, 3.96; N, 7.33; Cu, 16.62. Found: C, 37.7; H, 3.8; N, 7.1; Cu, 16.6

$Cu^{II}Cu^{I}L(ClO_4)$ was prepared in a helium atmosphere from the $Cu^{II}Cu^{II}$ complex by constant-potential electrolysis at −0.71 V. Details of the electrolysis cell and instrumentation are given earlier in this Experimental Section. The working compartment initially contained 0.35–0.40 g of the $Cu^{II}Cu^{II}$ species in DMF (25 mL). During the electrolysis the solution changed in color from green to blue-green. After completion of the electrolysis (n = 1.0 ± 0.1) the working compartment solution was transferred to a separate vessel and diethyl ether (50–75 mL) was added causing a dark brown solid to precipitate. After filtration the solid was dried and recrystallized from a saturated solution of boiling methanol, yielding dark brown needles which were dried in vacuo. Anal. Calcd for $C_{24}H_{26}N_4O_6ClCu_2$: C, 45.83; H, 4.17; N, 8.9; Cu, 20.20. Found: C, 45.6; H, 4.4; N, 8.7; Cu, 19.85.

$Cu^{II}Cu^{I}L(CO)ClO_4$ was synthesized using Schlenk techniques by the addition of carbon monoxide to solutions of the precursor mixed-valence complex, $Cu^{II}Cu^{I}L(ClO_4)$. Under a CO atmosphere solid $Cu^{II}Cu^{I}$ complex was dissolved in a minimum volume of DMF and the resulting solution was filtered. Diethyl ether, which was deaerated by bubbling with CO, was added slowly to the filtrate until a light brown solid precipitated. The solid was collected by filtration and dried under a stream of CO. Anal. Calcd for $C_{25}H_{26}N_4O_7ClCu_2$: C, 45.70; H, 3.99; N, 8.53; Cu, 19.34. Found: C, 45.9; H, 4.25; N, 8.65; Cu, 19.05.

$Cu^{I}Cu^{I}L$ was synthesized under a helium atmosphere from the $Cu^{II}Cu^{II}$ complex by constant-potential electrolysis at −0.71 V and then at −1.16 V. Initially, electrolysis was carried out at −0.71 V as described in the preparation of the $Cu^{II}Cu^{I}$ complex, $Cu^{II}Cu^{I}L(ClO_4)$. The solution was then further reduced at −1.16 V (n = 1.0 ± 0.1). During the latter process a dark brown, almost insoluble, powder formed which was collected and dried. The compound was redissolved in a small volume of DMF under a CO atmosphere, using Schlenk techniques. After filtration the CO was allowed to slowly (over a 48-h period) diffuse out of solution into an argon stream. Shiny black crystals formed which were collected and dried in vacuo. Anal. Calcd for $C_{24}H_{26}N_4O_2Cu_2$: C, 54.43; H, 4.95; N, 10.58; Cu, 24.00. Found: C, 54.1; H, 5.05; N, 10.75; Cu, 24.4.

$Zn^{II}Zn^{II}L(ClO_4)_2\cdot 2H_2O$. 1,3-Diaminopropane (0.5 mL, 6.0 mmol) followed by $Zn(ClO_4)_2\cdot 6H_2O$ (2.27 g, 6.1 mmol) in methanol (25 mL) were added to a solution of 5-methyl-2-hydroxyisophthalaldehyde (1.0 g, 6.1 mmol) in ethanol (100 mL) with stirring and mild heating. A yellow precipitate formed immediately on addition of the zinc salt but it quickly dissolved, giving a yellow solution. The solvent was evaporated to near dryness, with gentle heating, and was cooled to the ambient temperature. The resulting orange-yellow solid was isolated by filtration, then recrystallized from 1:1 ethanol/methanol to give a bright yellow, microcrystalline powder. Anal. Calcd for $C_{24}H_{30}N_4O_{10}Cl_2Zn_2$: C, 37.52; H, 3.94; N, 7.30; Zn, 17.02. Found: C, 37.7; H, 3.9; N, 7.0; Zn, 17.7.

Acknowledgment. We appreciate helpful discussions with Professors H. B. Gray and B. M. Hoffman. This work was suported by National Science Foundation Grant CHE76-82124 and by an Institutional Grant from the Department of Energy (EX-76-G03-1305).

References and Notes

(1) See ref 2–4 and references cited therein for examples of binuclear complexes derived from polydentate ligands.
(2) N. H. Pilkington and R. Robson, *Aust J. Chem.*, **23**, 225–236 (1970).
(3) M. D. Glick and R. L. Lintvedt, *Prog. Inorg. Chem.*, **21**, 233–260 (1976); S. E. Groh, *Isr. J. Chem.*, **15**, 277–307 (1977); G. R. Newkome, J. D. Sauer, J. M. Roper, and D. C. Hagar, *Chem. Rev.*, 77, 513–597 (1977).
(4) H. Okawa, V. Kasempimolporn, and S. Kida, *Bull. Chem. Soc. Jpn.*, **51**, 647–648 (1978); H. O. Okawa, U. Nishida, M. Tanaka, and S. Kida, *ibid.*, **50**, 127–131 (1977); H. Okawa, T. Tokii, Y. Nonaka, Y. Muto, and S. Kida, *ibid.*, **46**, 1462–1465 (1973); and references cited therein.
(5) R. R. Gagné, C. A. Koval, and T. J. Smith, *J. Am. Chem. Soc.*, **99**, 8367–8368 (1977).
(6) Abbreviations used in this paper include E^f, formal reduction potential; HMDE, hanging mercury drop electrode; TBAP, tetrabutylammonium perchlorate; DMF, *N,N*-dimethylformamide.
(7) R. N. Adams, "Electrochemistry at Solid Electrodes", Marcel Dekker, New York 1969, pp 144–145.

(8) L. Meites, "Polarographic Techniques", Wiley, New York, 1965, p 218.
(9) E. P. Parry and R. A. Osteryoung, *Anal. Chem.*, **37**, 1634–1637 (1965).
(10) R. R. Gagné, J. L. Allison, R. S. Gall, and C. A. Koval, *J. Am. Chem. Soc.*, **99**, 7170–7178 (1977).
(11) A. W. Addison, M. Carpenter, L. K-M. Lav, and M. Wicholas, *Inorg. Chem.*, 17, 1545–1552 (1978).
(12) G. C. Percy and D. A. Thornton, *J. Inorg. Nucl. Chem.*, **34**, 3357–3367 (1972).
(13) M. I. Bruce, *J. Organomet. Chem.*, **44**, 209–226 (1972); M. I. Bruce and A. P. Ostayewski, *J. Chem. Soc., Chem. Commun.*, 1124–1125 (1972); M. R. Churchill, B. G. DeBoer, F. J. Rotella, O. M. Abu Salah, and M. I. Bruce, *Inorg. Chem.*, **14**, 2051–2056 (1976); C. Meall, C. S. Arcus, J. L. Wilkinson, T. J. Marks, and J. A. Ibers, *J. Am. Chem. Soc.*, **98**, 711–718 (1976); R. R. Gagné, R. S. Gall, G. C. Lisensky, R. E. Marsh, and L. R. Speltz, *Inorg. Chem.*, **18**, 771–781 (1979); ref 10.
(14) E. F. Hasty, T. J. Colburn, and D. N. Hendrickson, *Inorg. Chem.*, **12**, 2414–2421 (1973).
(15) C. Sigwart, P. Hemmerich, and J. T. Spence, *Inorg. Chem.*, 7, 2545–2548 (1968).
(16) C. P. Slichter, *Phys. Rev.*, **99**, 478–480 (1955).
(17) Assuming that the triplet spectrum does arise from dipolar through-space coupling as a result of dimerization, the zero-field splitting and $g_\parallel$ parameters were used to calculate a Cu–Cu separation. The analysis was that used by Chang in studying confacial copper porphyrins.[18] The latter gave triplet EPR spectra essentially the same as that obtained for the dimer here. From the dimer spectrum $g_\parallel = 2.591$ and $2D_\parallel/g_\parallel\beta = 865$ G where $D_\parallel$ is the zero-field splitting and β is the Bohr magneton.[19] Solving for $D_\parallel$ gives a value of 0.0052 cm^{-1}. The Cu–Cu distance can be obtained from the relation[20] $r = (0.65g_\parallel^2/D_\parallel)^{1/3}$ giving 4.4 Å, which is comparable to the 4.2-Å separation found for the porphyrins.
(18) C. K. Chang, *J. Heterocycl. Chem.*, **14**, 1285–1288 (1977).
(19) C.-C. Chao and J. H. Lindsford, *J. Chem. Phys.*, **57**, 2890–2898 (1972).
(20) E. F. Hasty, L. J. Wilson, and D. N. Hendrickson, *Inorg. Chem.*, 17, 1834–1841 (1978).
(21) J. A. Huheey, "Inorganic Chemistry", Harper and Row, New York, 1972, p 259.
(22) I. M. Kolthoff and J. F. Coetzee, *J. Am. Chem. Soc.*, **79**, 1852–1858 (1957).
(23) B. F. Hoskins, R. Robson, and G. A. Williams, *Inorg. Chim. Acta*, **16**, 121–133 (1976).
(24) R. R. Gagné, T. Smith, and C. Koval, unpublished results.
(25) C. Creutz and H. Taube, *J. Am. Chem. Soc.*, **95**, 1086–1094 (1973).
(26) G. S. Patterson and R. H. Holm, *Bioinorg. Chem.*, **4**, 257–275 (1975).
(27) B. R. Reinhammar and T. I. Vänngård, *Eur. J. Biochem.*, **18**, 463–468 (1971); B. R. Reinhammar, *Biochim. Biophys. Acta*, **275**, 245–259 (1972).
(28) N. Makino, P. McMahill, and H. S. Mason, *J. Biol. Chem.*, **249**, 6062–6066 (1974).
(29) E. I. Solomon, D. M. Dooley, R. Wang, H. B. Gray, M. Cerdonio, F. Mogno, and G. L. Romani, *J. Am. Chem. Soc.*, **98**, 1029–1031 (1976).
(30) F. Ammar and J. M. Savéant, *J. Electroanal. Chem. Interficial Electrochem.*, **47**, 115–125 (1973); **47**, 215–221 (1973).
(31) D. S. Polcyn and I. Shain, *Anal. Chem.*, **38**, 370–375 (1966).
(32) R. L. Myers and I. Shain, *Anal. Chem.*, **41**, 980 (1969).
(33) J. B. Flanagan, S. Margel, A. J. Bard, and F. C. Anson, *J. Am. Chem. Soc.*, **100**, 4248–4253 (1978).
(34) J. Phelphs and A. J. Bard, *J. Electroanal. Chem.*, **68**, 313–335 (1976).
(35) W. H. Morrison, Jr., S. Krogsrud, and D. N. Hendrickson, *Inorg. Chem.*, **12**, 1998–2004 (1973).
(36) For example, see: R. E. Dessy, P. M. Weissman, and R. L. Pohl, *J. Am. Chem. Soc.*, **88**, 5117–5121 (1966); R. E. Dessy, R. Kornmann, C. Smith, and R. Haytor, *ibid.*, **90**, 2001–2004 (1968).
(37) N. H. Furman and G. Stone, *J. Am. Chem. Soc.*, **70**, 3055–3061 (1948).
(38) For example, see ref 25 and 39–41.
(39) R. W. Callahan, F. R. Keene, T. J. Meyer, and D. J. Salmon, *J. Am. Chem. Soc.*, **99**, 1064–1073 (1977).
(40) G. M. Tom, C. Creutz, and H. Taube, *J. Am. Chem. Soc.*, **96**, 7827–7829 (1974).
(41) T. R. Weaver, T. J. Meyer, S. A. Adeylmi, G. M. Brown, R. P. Eckberg, W. E. Hatfield, E. C. Johnson, R. W. Murray, and D. Untereker, *J. Am. Chem. Soc.*, **97**, 3039–3048 (1975).
(42) R. L. Lintvedt, B. Tomlonovic, D. E. Fenton, and M. D. Glick, *Adv. Chem. Ser.*, **32**, 407–425 (1975).
(43) $E_{1/2} = 0.995$ V vs. NHE; slope of $-E$ vs. log $i/(i_d - i)$ plot = 56.6 mV; CPE at −1.2 V yields an n value of 1.0 ± 0.1; R. R. Gagné, R. P. Kreh, and C. A. Koval, unpublished results.
(44) D. E. Fenton, R. R. Schroeder, and R. L. Linvedt, *J. Am. Chem. Soc.*, **100**, 1931–1932 (1978).
(45) A. W. Addison, *Inorg. Nucl. Chem. Lett.*, **12**, 899–903 (1976).
(46) M. B. Robin and P. Day, *Adv. Inorg. Chem. Radiochem.*, **10**, 247–422 (1967).
(47) N. S. Hush, *Prog. Inorg. Chem.*, **8**, 391–444 (1967).
(48) T. J. Meyer, *Acc. Chem. Res.*, 11, 94–100 (1978).
(49) M. J. Powers and T. J. Meyer, *J. Am. Chem. Soc.*, **100**, 4393–4398 (1978).
(50) W. H. Morrison and D. N. Hendrickson, *J. Chem. Phys.*, **59**, 380–386 (1973).
(51) W. H. Morrison and D. N. Hendrickson, *Inorg. Chem.*, **14**, 2331–2346 (1975).
(52) J. K. Beattie, N. S. Hush, and P. R. Taylor, *Inorg. Chem.*, **15**, 992, 993 (1976).
(53) B. C. Bunker, R. S. Drago, D. N. Hendrickson, R. M. Richman, and S. L. Kessell, *J. Am. Chem. Soc.*, **100**, 3805–3814 (1978).
(54) F. Basolo and R. G. Pearson, "Mechanisms of Inorganic Reactions," 2nd ed., Wiley, New York, 1968, p 454.
(55) R. R. Gagné, J. L. Allison, and G. C. Lisensky, *Inorg. Chem.*, 17, 3563–3571 (1978).
(56) The average EPR times scale was calculated using the hyperfine splitting for a low-temperature, isotropic four-line spectrum of $Cu^{II}Cu^{II}L^+$ where A_{av}, four was estimated as twice A_{av}, seven, Table IV. See: J. E. Wertz and J. R. Bolton, "Electron Spin Resonance", McGraw-Hill, New York, 1972, p 211.
(57) D. Lupu, D. Barb, G. Filott, M. Morariu, and D. Tarina, *J. Inorg. Nucl. Chem.*, **34**, 2803–2810 (1972).
(58) M. B. Robin, *Inorg. Chem.*, 1, 337–342 (1962).
(59) R. L. Belford, M. Calvin, and G. Belford, *J. Chem. Phys.*, **26**, 1165–1174 (1957).
(60) J. E. Bulkowski, P. L. Burk, M. F. Ludmann and J. A. Osborn, *J. Chem. Soc., Chem. Commun.*, 498–499 (1977).
(61) J. M. Lehn, S. H. Pine, E. Watanabe, and A. K. Willard, *J. Am. Chem. Soc.*, **99**, 6766–6768 (1977).
(62) A. H. Alberts, R. Annuziata, and J. M. Lehn, *J. Am. Chem. Soc.*, **99**, 8502–8504 (1977).
(63) R. R. Gagné, J. Dodge, and R. P. Kreh, manuscript in preparation.
(64) F. Ullmann and K. Brittner, *Chem. Ber.*, **42**, 2539–2548 (1909).
(65) D. Bauer and M. Breant, "Electroanalytical Chemistry", Vol. 8, A. J. Bard, Ed., Marcel Dekker, New York, 1975, pp 282–344.
(66) H. M. Koepp, H. Wendt, and H. Strehlow, *Z. Elektrochem.*, **64**, 483–491 (1960).